

Study of Spectral Characteristics, Kinetics, and Equilibria of Radicals Derived from Hydroxy Benzophenones

A. C. Bhasikuttan, A. K. Singh, D. K. Palit,* A. V. Sapre, and J. P. Mittal†

Chemistry Division, Bhabha Atomic Research Centre, Trombay, Mumbai, 400 085, India

Received: January 5, 1999; In Final Form: April 2, 1999

Studies on radical equilibria and the spectral evaluation have been carried out for three monohydroxy-substituted benzophenones (HOBP's) in aqueous solution. The transient ketyl or anion radicals were generated via hydrated electron (e_{aq}^-) reaction or dimethyl ketyl radical reaction in a pulse radiolysis experiment. The reactivity of both the undissociated (HOBP) as well as dissociated ($^-$ OBP) forms toward these reducing agents were studied. e_{aq}^- was found to react with the HOBP's and $^-$ OBP's with diffusion-controlled rates which are of the order $3 \times 10^{10} \text{ dm}^3 \text{ mol}^{-1} \text{ s}^{-1}$. In the case of the para derivative, two acid–base equilibria were identified (pK_a 9 and 11) in the pH range 6–13, one corresponding to the protonation–deprotonation at the OH site of the ketyl radical and the other for the protonation–deprotonation at the carbonyl site. For the ortho derivative, the intramolecularly hydrogen bonded structure of the radical anion has been found to be stable even in strongly alkaline solution (pH 13). Three different radical forms for the meta derivative have been identified at different pH conditions. The spectral evaluation of these radical species at different pH conditions was carried out. Reactions of dimethyl ketyl radicals with HOBP's and $^-$ OBP's were found to be different at different pH conditions. At acidic pH, it forms an adduct with the HOBP's, whereas at alkaline pH, the reaction with the ortho and meta derivatives occurs by H atom transfer. However, no reaction is seen with the para derivative in alkaline solution. Detailed spectral and kinetic data on the formation and decay of the various transient intermediates have been obtained.

1. Introduction

Photoreduction of the ketones and their derivatives in the presence of hydrogen atom donors is one of the widely investigated fundamental processes in photochemistry.^{1–8} It is now well established that in the photochemical reduction of the ketones in various solvents an intermediate step involves the reaction of the excited triplet state of the ketone with the solvent or another suitable hydrogen atom donor present in the solution to form the corresponding ketyl radical and free radical of the donor molecule. The excited triplet states of the ketones are capable of abstracting hydrogen atoms from a variety of substrates including hydrocarbons, alcohols, phenols, and amines.^{7,9–15} These reactions are known to occur by either a direct H atom transfer or an electron transfer mechanism followed by a proton transfer. However, it is evident that the efficiency of the photoreduction process is primarily dependent on the intersystem crossing (ISC) process from the singlet state of the ketone, i.e., the quantum yield of triplet state production, apart from the other factors, such as, the nature and electronic structure of the triplet state (i.e., whether it is $\pi\pi^*$ or $n\pi^*$ type) and the nature of the solvent.^{4,7,16–19}

The reactivity of the aromatic ketones toward hydrogen atom abstraction reaction has long been associated with the fundamental difference between the two kinds of triplet states, either $n\pi^*$ or $\pi\pi^*$, and this in turn is governed by the nature and position of the substituent in the aromatic ring and also by the solvent polarity.^{7,10,11,16} For example, the photochemical properties of benzophenone (BP) are known to be markedly affected by substitution.^{7,16,17,20,21} In alcoholic solvents, although the triplet of BP is known to abstract an H atom from the solvent

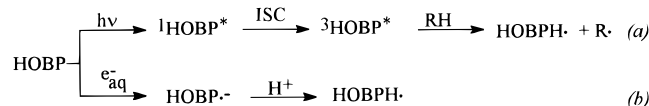
molecule in a facile way with a quantum yield of unity, for its amino and hydroxy derivatives, the quantum yields for the same process are much lower.^{20–22} Recently, we have investigated the photophysical properties and the photoinduced processes in ortho (*o*-), meta (*m*-), and para (*p*-) hydroxy benzophenones (HOBP's) using the technique of laser flash photolysis in the pico- and nanosecond time domain.²² It has been observed that the efficiencies of the ISC process for the HOBP's are far less than unity, particularly in polar hydrogen bond forming solvents. Among the hydroxy derivatives, *p*- and *m*-HOBP's are found to get photoreduced in hydrocarbon solvents with good yield, but not in alcohols. The quantum yield of the triplet for *o*-HOBP is only about 10% and is stable toward photoreduction in all kinds of solvents. Alcoholic solvents offer the possibility of hydrogen bond formation with HOBP's resulting in drastic differences between the photophysical and photochemical properties of the triplet states of such molecules.^{16d,22,23} Photoprocesses in *o*-HOBP are dominated by intramolecular hydrogen bonding, whereas for *p*-HOBP, intermolecular hydrogen bonding with the solvent seems to be important.^{22,24–27}

As mentioned above, in the process of photoreduction, ketyl radical is generated in the reaction between the triplet state and the hydrogen atom donor. The final products of the photoreduction process should depend on the nature of the triplet state and the reaction of the ketyl radical. However, for BP and many of its derivatives, the triplet states and the ketyl radicals absorb in the same wavelength region showing overlapping absorption bands^{22,28} and hence pose difficulties in studying the spectroscopic and kinetic behavior of these species by photochemical techniques. Moreover, the quantum yield of formation of the ketyl radical on photolysis of the ketone depends on the efficiencies of the ISC process, which is very low for the hydroxy derivatives of benzophenone,²² and also the rate of the H atom abstraction reaction by the triplet is low.

* Author for correspondence.

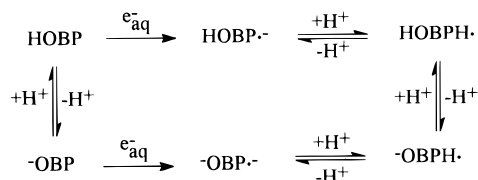
† Also affiliated as Honorary Professor with The Jawaharlal Nehru Centre for Advanced Scientific Research, Bangalore, India.

The electron pulse radiolysis technique, which is complementary to the flash photolysis technique, has been used effectively for studying the properties of the ketyl radicals.^{29,30} An advantage of this technique is that the ketyl radical is formed by protonation of the radical anion of the ketone thus avoiding the intermediacy of the triplet state. The ketyl radicals are formed in good yield because the parent ketones have high reactivities toward solvated or hydrated electrons (*vide infra*).



The two routes are given in reactions a and b. The former is followed in the photoinduced reaction, while the latter occurs in electron pulse radiolysis.

In this study, using electron pulse radiolysis, an attempt is made to study the equilibria as given below and obtain the spectroscopic and kinetic properties of the various radical species produced from the three monohydroxy-substituted benzophenones (HOBP), namely, *ortho*-, *meta*-, and *para*-HOBP.



2. Experimental Section

o-, *m*-, and *p*-HOBP's were purchased from Aldrich Chem. Co., USA. The *para* and *meta* derivatives were further purified from ethanol–water mixtures, whereas the *ortho* derivative was purified by vacuum sublimation. Solvents used, e.g., *tert*-butyl alcohol, 2-propanol, and acetone, were of spectroscopic grade and were used without further purification. Buffer solutions were prepared from the suitable mixtures of solutions of Na₂HPO₄ and NaH₂PO₄ mixtures. All aqueous solutions were prepared in Nanopure water obtained from a Barnstead System (resistivity 18.3 MΩ cm).

A detailed experimental set up for the electron pulse radiolysis and the kinetic spectrophotometry has been described elsewhere.³¹ Sample solutions taken in a suprasil cuvette of 1 cm path length were irradiated by electron pulses of 50 ns duration (fwhm) from a 7 MeV linear electron accelerator (Ray Technology, England) at a radiation dose of 10–12 Gy per pulse as measured by an air-saturated 0.05 mol dm⁻³ KCNS dosimeter, taking *G*ε for (CNS)₂^{•-} as 21 522 dm³ mol⁻¹ cm⁻¹ at 500 nm (*G* being defined as number of molecules formed per 100 eV energy absorbed).^{32a} The transient absorption profiles were monitored by a kinetic spectrophotometric arrangement consisting of a 450 W pulsed xenon lamp in conjunction with a monochromator (CVI model 110) and photomultiplier tube (Hamamtsu R 928), connected to a digital oscilloscope (L&T Gould 4072). The data were transferred to an IBM PC where data analysis was carried out.

3. Results and Discussion

3.1. Ground-State Acid–Base Equilibria. A prior understanding of the ground-state acid–base equilibria relating to the dissociation of the OH group of the HOBP's is essential to understand the reactions and the decay kinetics of the transients produced following reactions with the hydrated electron (e_{aq}⁻)

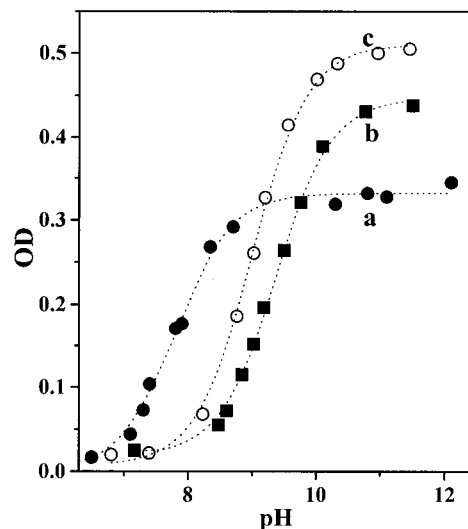
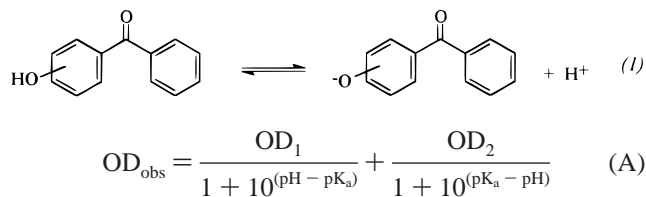
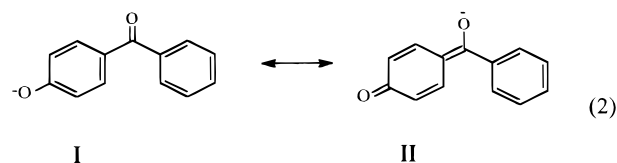


Figure 1. Changes in absorbance at the absorption maximum of the anion (⁻OBP) as a function of pH in case of *p*-HOBP (a), *o*-HOBP (b), and *m*-HOBP (c). The dotted lines represent the fitting curves obtained following eq A.

and other reducing radicals used in the present work. For this purpose, ground-state spectra of HOBP's have been studied in aqueous solutions as a function of pH. The anions (⁻OBP's) of *o*-, *m*-, and *p*-HOBP, which are stable at higher pH (e.g., pH ≈ 12), absorb with λ_{max} at 380, 360, and 345 nm, respectively. Absorbance values of the ⁻OBP's have been monitored at these wavelengths and plotted as a function of pH (Figure 1) and the p*K*_a values for the equilibria (reaction 1) have been obtained by fitting the sigmoid curves to eq A.³³



where OD₁ and OD₂ represent the absorbance values at a suitable wavelength due to undissociated and dissociated forms, respectively. The p*K*_a values thus estimated are 7.9 ± 0.1, 9.0 ± 0.1, and 9.3 ± 0.1 for *p*-, *m*-, and *o*- derivatives, respectively. The higher value of the p*K*_a for hydrogen ion dissociation in the case of *o*-HOBP is easily evident from its ability to form strong intramolecular hydrogen bonds.^{24–27} Among the other two derivatives, the lower value of p*K*_a for *p*-HOBP can be explained due to the highly stabilized charge-transfer type valence bond structure of *p*-⁻OBP (**I** and **II**) which is not possible in the case of the *meta*-derivative.



3.2. Reaction of e_{aq}⁻. Radiolysis of water generates three major primary reactive species, e_{aq}⁻, OH[•], and H[•] with *G* values 2.7, 2.7, and 0.5, respectively. The *G* value for e_{aq}⁻ is constant (2.7) in the pH range 4–10.^{34a} Although no data is being reported here for pH < 4, a few experiments have been performed in solutions with pH > 10 at which *G*(e_{aq}⁻) is greater

TABLE 1: Transient Characteristics of the Radical Species Generated in the Reaction of e_{aq}^- with the HOBP's

compound	species	λ_{max} (nm)	ϵ_{max} (dm ³ mol ⁻¹ cm ⁻¹)	$k(e_{aq}^-)$ (dm ³ mol ⁻¹ s ⁻¹)	$2k$ (dm ³ mol ⁻¹ s ⁻¹)	pK _a	
						HOBP	radical
<i>p</i> -HOBP	<i>p</i> -HOBPH [•] (V)	545	3300	$(3.13 \pm 0.2) \times 10^{10a}$	2×10^9	7.9 ± 0.1^c	9.1 ± 0.1 (V \rightleftharpoons VII)
	<i>p</i> ⁻ OBPH [•] (VII)	565	4000				11.1 ± 0.1 (VII \rightleftharpoons VI)
	<i>p</i> -OBP ^{2•-} (VI)	600	4630	$(3.0 \pm 0.2) \times 10^{10b}$	9.2×10^8		
<i>o</i> -HOBP	<i>o</i> -HOBPH [•] (X)	550	2300	$(3.14 \pm 0.3) \times 10^{10a}$	6.9×10^9	9.3 ± 0.1^c	6.9 ± 0.1 (X \rightleftharpoons IX)
	<i>o</i> -OBPH [•] (IX)	600	4850	$(2.65 \pm 0.15) \times 10^{10b}$	1.65×10^9		
<i>m</i> -HOBP	<i>m</i> -HOBPH [•] (XIV)	550	2800	$(4.12 \pm 0.3) \times 10^{10a}$	1.7×10^9	9.0 ± 0.1^c	6.5 ± 0.1 (XIV \rightleftharpoons XIII)
	<i>m</i> -OBP ^{2•-} (XVII)	610	5700	$(3.25 \pm 0.2) \times 10^{10b}$	9.4×10^8		8.5 ± 0.1 (XIII \rightleftharpoons XVII)

^a Rate constant for $e_{aq}^- + \text{HOBP}$ at pH 5.6. ^b Rate constant for $e_{aq}^- + \text{OBP}$ at pH 11. ^c Ground-state acid–base equilibrium.

than 2.7, and in such cases, the actual values of $G(e_{aq}^-)$ reported at the respective pH's have been used.^{34a} Among the three primary species, OH[•] is the oxidizing species, while the other two are reducing in nature. By adding suitable scavengers in the solution, the reaction conditions can be adjusted in such a way that only the reaction of e_{aq}^- with the solutes can be exclusively studied. The kinetics of the reaction of e_{aq}^- with the HOBP's were studied in deaerated aqueous solutions of different concentrations (varying from 2.5×10^{-5} mol dm⁻³ to 2×10^{-4} mol dm⁻³) of the HOBP's containing ~ 1 mol dm⁻³ of *tert*-butyl alcohol. *tert*-Butyl alcohol scavenges the oxidizing OH[•] radical efficiently and also increases the solubility of the HOBP's in aqueous solutions. The decay of e_{aq}^- was monitored at 720 nm in the presence of the HOBP's at different pH conditions. From the plot of the pseudo-first-order rate constants vs the HOBP concentrations, the second-order rate constant values have been evaluated for all the three HOBP's and have been given in Table 1. All three HOBP's and ⁻OBP's are found to be very reactive toward e_{aq}^- , and the rate constants are of the order of $\sim 3 \times 10^{10}$ dm³ mol⁻¹ s⁻¹ (Table 1). Considering the fact that the >C=O group is the most electron affinic center in the HOBP or ⁻OBP molecule, it is evident that the electron is captured by the molecule to produce the anion radical species as the primary reaction product. The fate and the subsequent reactions of this anion radical species have been found to depend on the pH of the solution and the position of the OH group in the phenyl ring, and this will be discussed in the following sections.

p-HOBP. Spectral characterization and the decay kinetics of the anion radical species produced due to the reaction of e_{aq}^- with *p*-HOBP (2×10^{-3} mol dm⁻³) in aqueous solutions of different pH's has been presented in Figure 2. At this concentration of *p*-HOBP (and also the other two HOBP's) used, the reaction with e_{aq}^- is complete within 300 ns, as seen from the decay of the hydrated electron monitored at 720 nm (trace 1, inset of Figure 2B). Hence, the spectra of the anion radical species being reported here have been recorded at 400 ns after the electron pulse.

Figure 2A shows the time-resolved transient absorption spectra recorded in solution buffered at pH 6 soon after the electron decay (i.e., at 400 ns) and at 4 μ s after the electron pulse. At this pH, *p*-HOBP exists in undissociated form (III). The early-time spectrum a has a peak at 540 nm and a shoulder at 620 nm. The absorbance in the 600–700 nm region has been seen to decay faster, and the resultant spectrum b recorded at 4 μ s is very similar to that of ketyl radical of *p*-HOBP (V) reported earlier.²² The spectrum a recorded at 400 ns after the pulse can be attributed to a mixture of the anion radical (IV) formed due to electron addition and the ketyl radical (V), which has subsequently been formed due to protonation of the precursor anion radical (reaction 3). With the protonation reaction being very fast, within 400 ns, an appreciable amount of the species V has been formed due to protonation of its precursor species IV (Scheme 1).

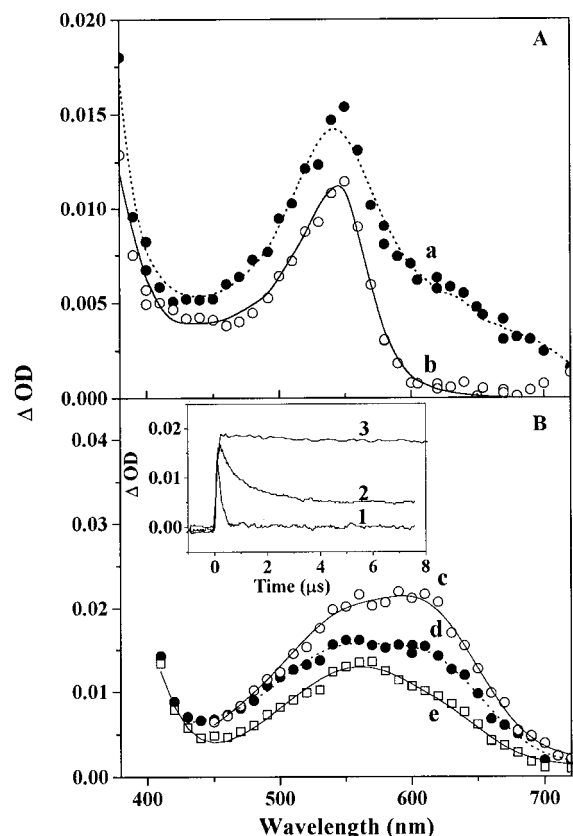
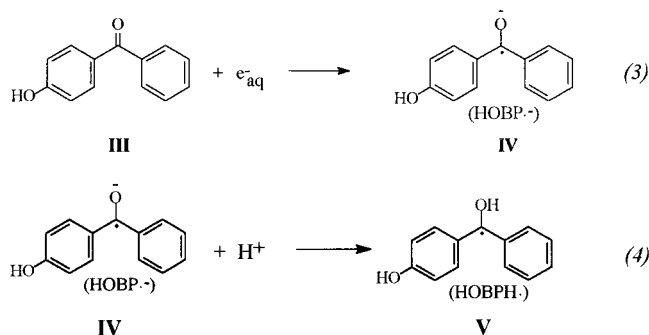


Figure 2. Time-resolved absorption spectra of the transient radical species produced due to reaction of e_{aq}^- with *p*-HOBP in aqueous solution: (A) at pH 6.2 recorded at 400 ns (a) and 4 μ s (b) after the pulse; (B) pH 13 recorded at 400 ns (c) and pH 10.5 recorded at 400 ns (d) and 4 μ s (e) after the pulse. Inset shows the kinetic traces recorded at 720 nm (1) and 610 nm (2) in the solution at pH 10.5 and at 610 nm (3) in the solution at pH 13.

SCHEME 1



The absorption spectrum c in Figure 2B is due to the only transient produced in the reaction of e_{aq}^- with *p*⁻OBP at pH 13. As the pK_a of the ground state of *p*-HOBP is 7.9, it is evident that, at pH 13, *p*-HOBP exists exclusively in the deprotonated form, *p*⁻OBP (I) and the generation of the transient anion

SCHEME 2

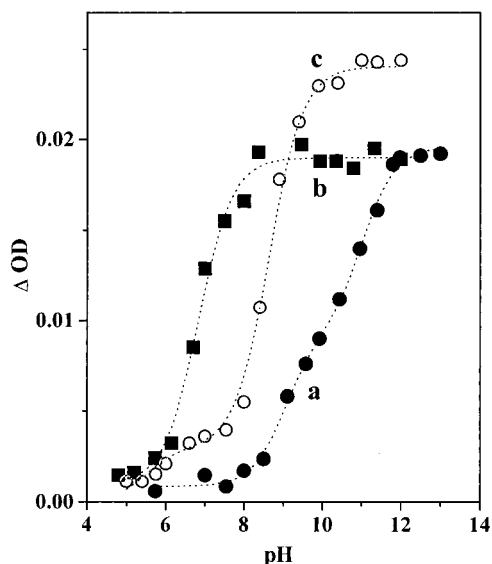
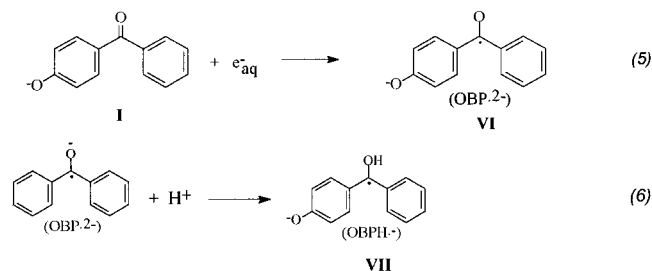


Figure 3. Absorbance changes recorded at 610 nm as a function of pH on radiolysis of aqueous solution containing $1 \times 10^{-3} \text{ mol dm}^{-3}$ of HOBP, 1 mol dm^{-3} *tert*-butyl alcohol, saturated with N_2 : *p*-HOBP (a); *o*-HOBP (b); *m*-HOBP (c). The dotted line represents the fitting according to eq B.

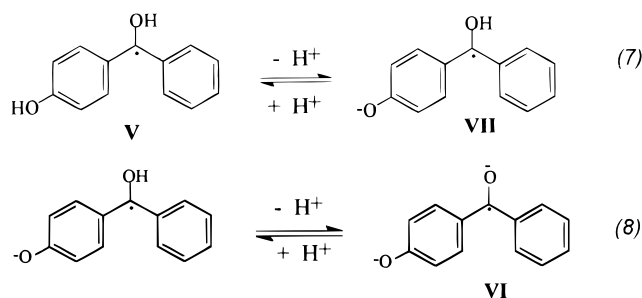
radical species **VI** due to the reaction of e_{aq}^- with the *p*-OBP can be represented by eq 5 (Scheme 2). The transient absorption spectrum *c* shows a broad band in the wavelength region 450–700 nm, and the transient decay monitored at different wavelengths on the absorption band indicates that the band is due to a single species. The anion radical species **VI** is long-lived, and the decay rate is given in Table 1.

To obtain the acid–base dissociation constants for the ketyl-anion radical equilibrium ($\text{VII} \rightleftharpoons \text{VI}$), the absorbance values of the radical ion species surviving at $4 \mu\text{s}$ after the electron pulse were measured as a function of pH at 610 nm (Figure 3a). The absorbance values show a gradual increase when the pH is increased from 6 to 14. It is important to note that, although above pH 10 only the *p*-OBP species exists in solution, the absorbance of the transient radical species gradually increases with pH in the range 10 to 13. As a result, the transient absorbance vs pH curve in the pH range 6–14 appears to be a combination of two sigmoidal curves indicating two acid–base equilibria of the radical species produced due to reaction of e_{aq}^- with *p*-OBP, one in the pH range 8–10 and the other in the pH range 10–13.

Spectra *d* and *e* in Figure 2B are due to the transient radical species produced after e_{aq}^- addition to *p*-OBP at pH 10.5 and recorded at 400 ns and $4 \mu\text{s}$ after the electron pulse. Also, the inset of Figure 2B shows the decay trace of the radical species at 610 nm (trace 2). The decay trace 2 shows a fast component which decays to another slow component within $4 \mu\text{s}$. The spectrum of the transient radical species recorded at $4 \mu\text{s}$ after

the electron pulse (spectrum *e*) is distinctly different from that of the anion radical species **VI**. Comparing the decay traces recorded at 610 nm at pH 10.5 and 13 (traces 2 and 3, respectively, in the inset of Figure 2B), it can be said that the initial decay seen in trace 2 is due to the protonation reaction of the initial electron adduct (species **IV**). The protonation occurs at the carbonyl site (reaction 6), and spectrum *e* in Figure 2B can be assigned to species **VII**. The lower absorbance value in spectrum *d* as compared to that in spectrum *c* is evident as the $G(e_{\text{aq}}^-)$ is less at pH 10.5 than that at pH 13. Also, the protonation reaction is fast and is complete to some extent before 400 ns, at which time spectrum *d* has been recorded.

Having identified the different transient radical species produced due to electron reactions with *p*-HOBP at different pH's, two different acid–base equilibria can be identified for the sigmoidal pK_a curve (Figure 3a). These are represented in reactions 7 and 8. The one in the pH range 8–10 involves the protonation–deprotonation at the phenolic OH site (reaction 7) and the other in the pH range > 10 can be assigned to the reaction 8, i.e., due to the protonation–deprotonation at the carbonyl site.



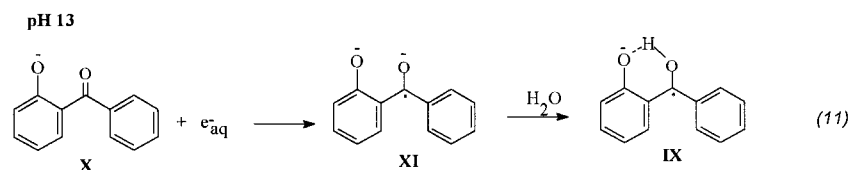
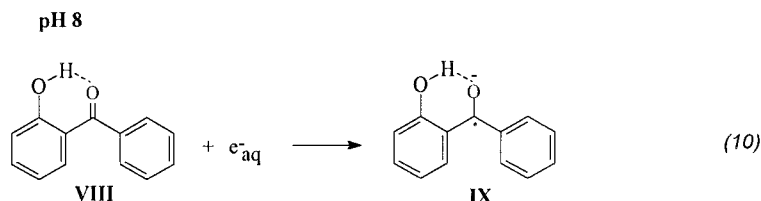
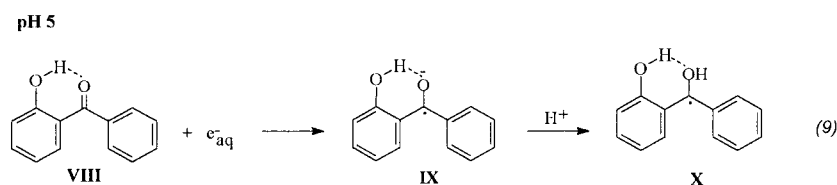
Considering these two equilibria reactions, (7) and (8), the measured absorbance of the transient radical species in solutions at different pH has been correlated by the following equation:³⁵

$$\text{OD}_{\text{obs}} = \frac{\text{OD}_{\text{V}}}{1 + 10^{(\text{pH} - \text{pK}_1)} + 10^{(2\text{pH} - \text{pK}_1 - \text{pK}_2)}} + \frac{\text{OD}_{\text{VII}}}{1 + 10^{(\text{pK} - \text{pH})} + 10^{(\text{pH} - \text{pK}_2)}} + \frac{\text{OD}_{\text{V}}}{1 + 10^{(\text{pK}_2 - \text{pH})} + 10^{(\text{pK}_1 + \text{pK}_2 - 2\text{pH})}} \quad (\text{B})$$

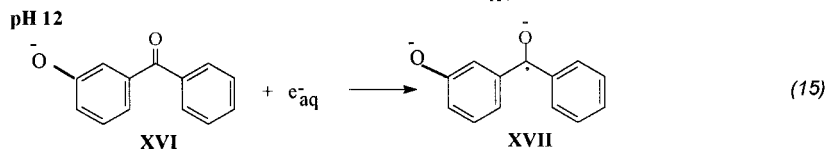
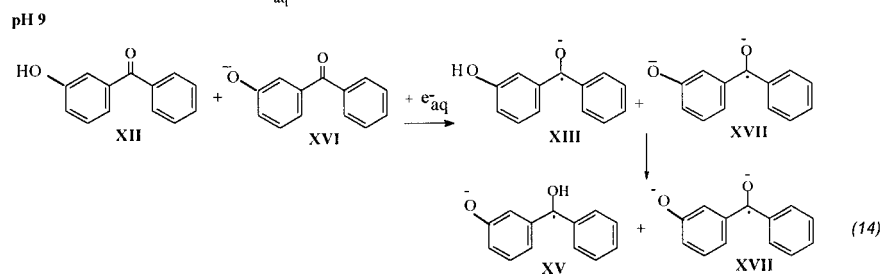
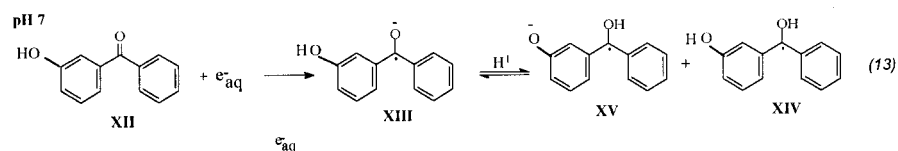
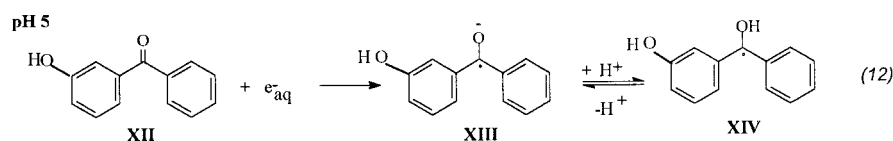
Here, OD_{V} , OD_{VI} , and OD_{VII} represent the optical densities of the species **V**, **VI**, and **VII**, respectively, at 610 nm at the pH where these are the only absorbing species in the solution. By knowing the values of OD_{V} and OD_{VI} at the two extreme pH values, the absorbance values plotted in Figure 3a were fitted to eq B. The dotted line represents the fit according to eq B giving pK_1 and pK_2 as 9.1 ± 0.1 and 11.1 ± 0.1 , respectively. Thus, the pK_a value of 9.1 corresponds to the pK_a for the phenolic OH of the ketyl radical (**V**) and the value of 11.1 corresponds to the pK_a at the carbonyl site of species **VII**. The higher pK_a value for the deprotonation of the OH at the carbonyl site of the ketyl radical (species **V**) as compared to that of benzophenone (pK_a 9.2)^{30a} can be explained by the fact that the release of a proton from the anion radical **VII** may not be a favorable process, possibly due to highly stabilized charge-transfer type valence bond structure (**II**).

o-HOBP. Reaction of e_{aq}^- with *o*-HOBP has been studied in deaerated aqueous solutions containing $1 \times 10^{-3} \text{ mol dm}^{-3}$ of *o*-HOBP and 1 mol dm^{-3} of *tert*-butyl alcohol buffered at

SCHEME 3



SCHEME 4



different pH's and the spectral and decay characteristics of the different radical species generated have been presented in Figure 4. Spectra a and b are due to the transient species produced due to addition of e_{aq}^- with *o*-HOBP in a solution at pH 5 and recorded at 400 ns and 4 μ s after the electron pulse, respectively. Keeping in mind the fact that the pK_a of the ground state of *o*-HOBP is 9.3, at pH 5 it exists as the species VIII in solution and the anion radical species IX is formed due to electron addition to *o*-HOBP (reaction 9). However, species IX undergoes fast protonation to form the ketyl radical species X. Spectrum b can be assigned to the latter, and spectrum a must be due to a mixture of the species IX and X. It has not been possible to record the correct absorption spectrum of the species IX because of the survival of e_{aq}^- in solution up to 300 ns after

the pulse and fast protonation of the species. Spectra c and d in Figure 4 represent the spectrum of the only transient radical species produced due to reaction of e_{aq}^- with *o*-HOBP at the pH's 8 and 13, respectively. Similarities in the spectra recorded at 400 ns and 4 μ s after the electron pulse at both the pH's and the nature of the decay traces (traces 2 and 3 in inset of Figure 4) indicate that the only radical species produced on electron addition does not undergo protonation or deprotonation to produce any other radical species. The initial little decay seen in traces 2 and 3 can be assigned due to that of e_{aq}^- (see trace 1 in inset of Figure 4). The absorbance values of the radical species present at 4 μ s after the electron pulse measured at 610 nm have been plotted as a function of the pH of the solutions in Figure 3b. The curve indicates a single pK_a (6.9) throughout

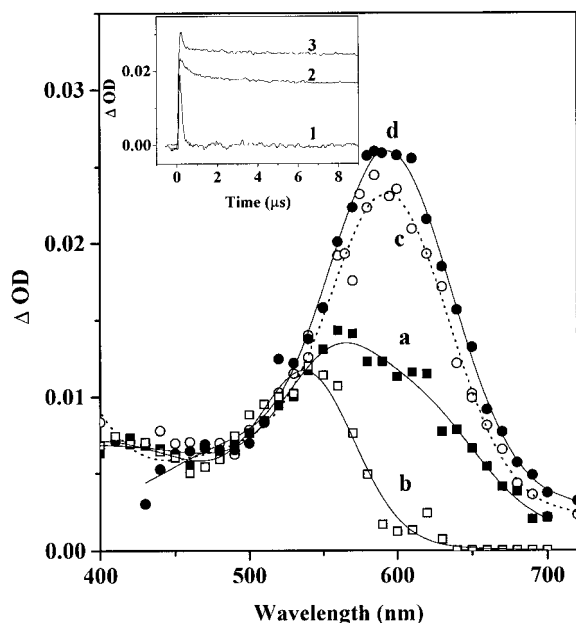


Figure 4. Time-resolved transient absorption spectra recorded in deaerated aqueous solution containing 1×10^{-3} mol dm^{-3} *o*-HOBP, 1 mol dm^{-3} *tert*-butyl alcohol. (a) and (b) represent the spectra obtained at 400 ns and 4 μs after the electron pulse in the above solution buffered at pH 5. (c) represents the spectrum recorded at 400 ns in the solution buffered at pH 7.5. (d) represents the spectrum recorded at 400 ns in the solution buffered at pH 12. (inset) Kinetic traces recorded at 720 nm (1) and 610 nm in the solutions at pH 8 (2) at pH 12 (3).

the pH range 5–12. Considering these experimental observations, the reactions have been summarized as in Scheme 3.

Scheme 3 shows the formation of the same radical species at both pH's, 8 and 13. At pH 8, the anion radical species **IX** formed on electron addition to *o*-HOBP, which exists as the species **VIII** at this pH, is exceptionally stable due to formation of intramolecular hydrogen bond. At pH 13, the anion radical species **XI**, formed due to addition of electron to *o*-OBP (**X**), undergoes very fast protonation to form the very stable species **IX**. However, our time-resolved spectra recorded at 400 ns after the pulse did not indicate any spectral change corresponding to this process. The lower value of the pK_a (6.9) for the ketyl radical (**XI**) indicates its stability. The spectral and the kinetic parameters of the transient radical species described above are given in Table 1.

m-HOBP. The spectral characteristics of the radical species produced due to reactions of e_{aq}^- with *m*-HOBP in solutions buffered at pH's 5, 7, 9 and 13 are presented in Figure 5 and Scheme 4 can be put forth to explain the sequence of formation of the different radical species at different pH's.

With the pK_a of the ground state of *m*-HOBP being 9.0, at pH's 5 and 7 it exists in the undissociated form **XII**. However, Figure 5 indicates that the characteristics of the absorption spectra of the transient radical species formed are different at these two pH conditions. Scheme 4 reveals that the anion radical species **XIII** formed due to electron adduct to *m*-HOBP and detected at 400 ns after the electron pulse should be the same, but spectra a and c in Figure 5 are different in nature. This is probably due to the fact that at pH 5, with the H^+ ion concentration being higher than that at pH 7, species **XIII** undergoes a very fast protonation reaction to produce the ketyl radical species **XIV** (spectrum b). But at pH 7 we are able to observe the actual spectrum of the anion species **XIII** at 400 ns after the electron pulse. However, a careful comparison between spectra b and d indicates some differences in their

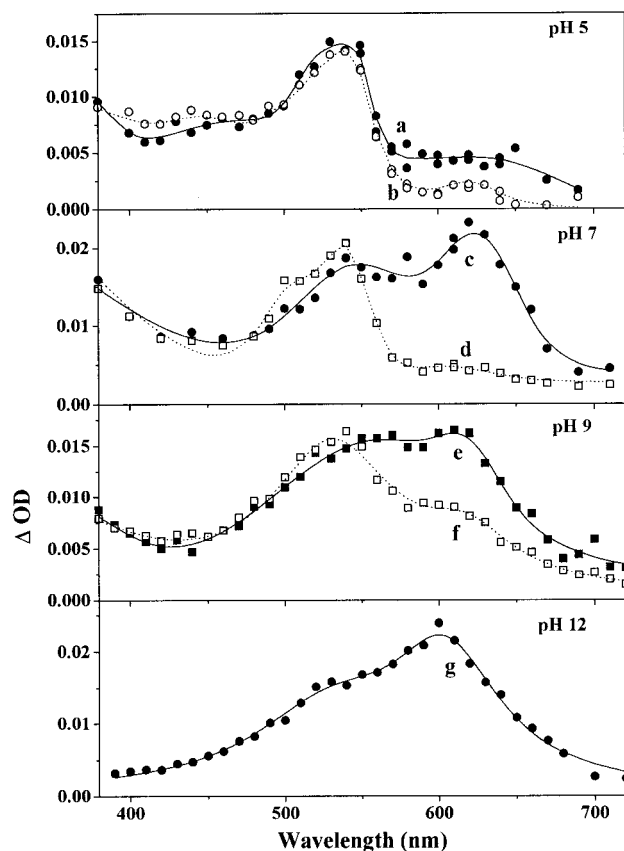
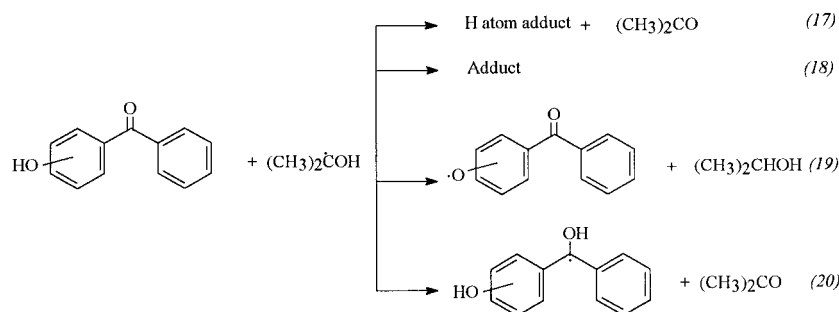


Figure 5. Time-resolved absorption spectra of the transient radical species produced due to reaction of e_{aq}^- with *m*-HOBP in aqueous solution at pH's 5, 7, 9, and 12 recorded 400 ns (a) and 4 μs (b) after the electron pulse.

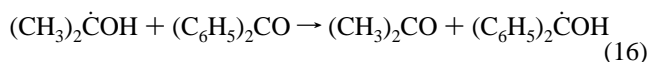
characteristics, although the gross features are the same (discussed later). At pH 12, *m*-HOBP exists in the dissociated form **XVI**. On electron addition to species **XVI**, anion radical species **XVII** is formed, and it does not undergo protonation to form any other species, as indicated by the similarity of spectra at 400 ns and 4 μs (spectrum g in Figure 5). Figure 3c shows the nature of the pK_a curve of the transient radical species in the pH range 5–13. It reveals the existence of two pK_a 's, one is at about 6.5 and the other one at about 8.5. The minor differences in spectra b and d recorded at pH 5 and 7 are probably explainable by the fact that, while at pH 5 the existing radical is the species **XIV** (spectrum b), the observed spectrum (d) at pH 7 is due to a mixture of two species, **XIV** and **XV**. We have also studied the nature of the transient radical species at pH 9. At this pH, *m*-HOBP exists as a mixture of undissociated (**XIII**) and dissociated (**XVI**) forms. Hence, at 400 ns after the electron pulse, the observed spectrum e is a mixture of species **XIII** and **XVII**, and the species **XIII** undergoes a proton-transfer reaction to form **XV**. Thus, at 4 μs after the electron pulse, the recorded spectrum f is a mixture of species **XV** and **XVII**. It should be noted that the radical species **XIII**, **XIV**, **XV**, and **XVII** have peak maxima at 620, 540, 540, and 600 nm, respectively.

3.3. Extinction Coefficient and Decay Kinetics of the Radical Species. The molar extinction coefficient of the transient radicals has been estimated by knowing the concentration of the reactive species generated during the electron pulse. This has been calculated by using thiocyanate as a dosimeter and measuring the absorbance of $(\text{SCN})_2^{\bullet-}$ at 500 nm. Assuming complete reaction with e_{aq}^- ($G_{e_{\text{aq}}^-} = G_{\text{radical}}$), the molar extinction coefficients for the ketyl radicals of HOBP and $^-$ OBP

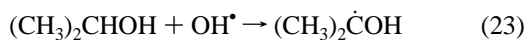
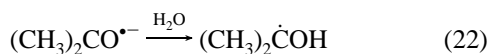


have been evaluated at 545 and 610 nm, respectively, and are given in Table 1. These values are close to that of the ketyl/anion radical of benzophenone reported earlier from radiolysis experiments.³⁶ The radical decays were monitored at their respective absorption maxima. The decay traces follow good second-order kinetics, and the rate constant values are tabulated in Table 1.

3.4. Reaction with Dimethyl Ketyl Radicals. Dimethyl ketyl radical is another specific reductant which reacts with BP to give diphenyl ketyl radical.³⁷ The aliphatic to aromatic radical transformation can be expressed as



In the present context, it will be of interest to see whether $(\text{CH}_3)_2\dot{\text{C}}\text{OH}$ radical attacks the $-\text{OH}$ group in HOBP to give phenoxy radical by an H abstraction process or attacks at the $>\text{C}=\text{O}$ site to reduce HOBP to give the ketyl radical. The possible reaction channels can be represented as in eqs 17–20. In pulse radiolysis experiments, $(\text{CH}_3)_2\dot{\text{C}}\text{OH}$ radicals are conveniently generated in good yield in aqueous 2-propanol–acetone mixed solvent (5 mol dm^{-3} 2-propanol, 1 mol dm^{-3} acetone in water) system which has been successfully used in the studies of several quinones.³⁵ In this system, as the composition of the mixed solvent system is 32.2 mol dm^{-3} water besides 6 mol dm^{-3} of total organic solvents, the bulk of the medium remains essentially aqueous and the principles of radiation chemistry of water can be fully applied including reporting of pH in these solutions. The advantage of such a mixed aqueous–organic solvent system mixture is that dimethyl ketyl radical can be generated quantitatively in a deoxygenated solution following the reactions represented below



Thus, both the oxidizing and reducing radicals give the same dimethyl ketyl radical with a yield of $G = 6.2$. This radical with a reduction potential of 1.1 V can be used to obtain selective reduction by either an H-atom transfer or electron-transfer process. $(\text{CH}_3)_2\dot{\text{C}}\text{OH}$ radical has a $\text{p}K_{\text{a}}$ equal to 12,³⁸ and its reactions can be conveniently studied below pH 11.

Following the generation of dimethyl ketyl radicals in a mixed aqueous–organic solvent system, its reaction with p -HOBP was studied. The transient spectra, obtained in the mixed solvent system containing 1×10^{-3} mol dm^{-3} of p -HOBP at pH 5, displayed an absorption band below 400 nm with a maximum at ~ 350 nm and is shown in Figure 6a. Surprisingly, we could not observe any absorption corresponding to the formation of

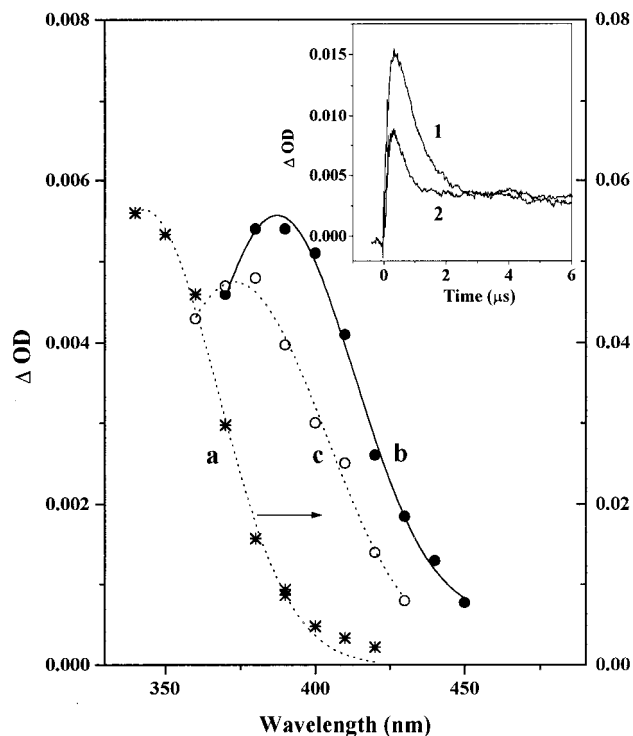


Figure 6. Transient absorption spectra obtained in deaerated mixed aqueous–organic solutions containing 1×10^{-3} mol dm^{-3} HOBP below their $\text{p}K_{\text{a}}$ values: *para*- (a), *ortho*- (b), and *meta*-HOBP (c). (inset) Absorbance profile recorded at 370 nm at pH 5.8 (1) and 6.5 (2) in the case of *p*-HOBP.

ketyl radical of p -HOBP in the region 400–800 nm (reaction 20). Also, there was no indication for the reduction of p -HOBP by dimethyl ketyl radical when the pH of the solution was increased to ~ 10 since we did not observe any transient absorption in the 400–800 nm region and, due to strong ground-state absorption of the alkaline solution, transient spectrum below 400 nm region could not be recorded. It is to be noted here that the transient spectrum obtained at pH 5 shows good spectral match with that of the phenolate ion (^-OBP),²² though the generation of this species in this reaction is doubtful. The absence of the ketyl radical of p -HOBP suggests that the reaction may proceed either by an H atom transfer to the ring (H atom adduct, reaction 17) or by hydrogen atom abstraction from the phenolic OH of the p -HOBP by the dimethyl ketyl radicals to give phenoxy radicals (reaction 19) or by adduct formation (reaction 18). To look for the possibility of formation of the H atom adduct, H atom reactions were exclusively followed in a solution containing 1×10^{-3} mol dm^{-3} of p -HOBP, 1 mol dm^{-3} *tert*-butyl alcohol, saturated with N_2 at pH 2. At this pH, e_{aq}^- gets converted to H atom and the OH radical is scavenged by *tert*-butyl alcohol. Interestingly, the transient spectrum obtained from H atom reaction (Figure 7a) is quite different from that

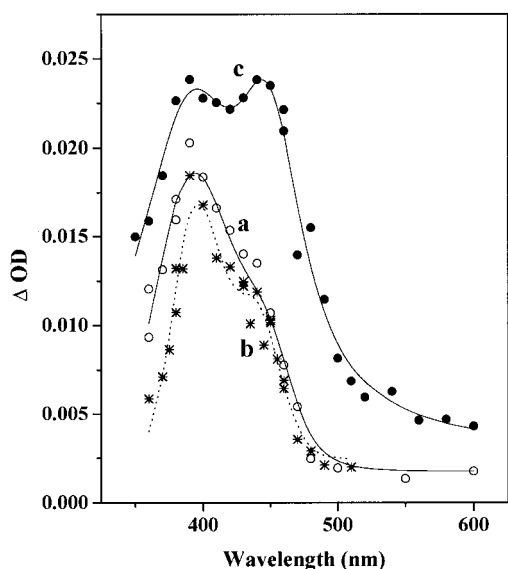


Figure 7. Transient absorption spectra recorded at 3 μs after the electron pulse in deaerated aqueous solutions containing the HOBP ($1 \times 10^{-3} \text{ mol dm}^{-3}$) and 1 mol dm^{-3} *tert*-butyl alcohol at pH 2: *para*- (a), *ortho*- (b), and *meta*-HOBP (c).

obtained from the reaction of dimethyl ketyl radical at pH 5. On the other hand, phenoxy radicals, in general, have very low pK_a values (<1)³⁹ and should not be sensitive to a change in pH from 6 to 7. However, the transient decay monitored at 370 nm for the above reaction at pH 6 and 6.5 (inset of Figure 6) clearly indicates a pH-dependent decay. These observations led us to attribute the transient absorption observed in acidic pH due to adduct formation between dimethyl ketyl radicals and *p*-HOBP (reaction 18). Dimethyl ketyl radicals are known to form adducts with the reactants and have been reported earlier in the case of some aromatic molecules.^{32b,40} A likely position for the addition of dimethyl ketyl radical would be at the more electropositive carbon in the benzene ring or at the $>\text{CO}$ group, which is a known center for reduction. However, from our data, it is not possible to distinguish between the two structures. It may happen that the absorption of the adduct is strong in alkaline solutions. Lack of reactivity of *p*-HOBP toward $(\text{CH}_3)_2\dot{\text{C}}\text{OH}$ at pH 10 ($k < 10^5 \text{ dm}^3 \text{ mol}^{-1} \text{ s}^{-1}$ which has been estimated from the competition between the self-decay of $(\text{CH}_3)_2\dot{\text{C}}\text{OH}$ ^{34b} and its reaction with *p*-HOBP) is probably due to high stability of the undissociated form ^-OBP (species **I** and **II**).

In the case of the *ortho* and *meta* derivatives too, the transient absorption spectra recorded in the deaerated mixed aqueous–organic solvent at pH ~ 6.5 show absorption bands with λ_{max} at 390 and 370 nm, respectively having no ketyl radical or anion radical absorption in the 500–600 nm region (parts b and c of Figure 6) and are attributed to the adduct formation. In these cases also, the data on the H atom reaction carried out at pH 2 (Figure 7) confirm that the reaction of dimethyl ketyl radical with *o*-HOBP does not occur through H atom transfer to the aromatic ring. As the signal is weak, detailed analysis could not be done.

The transient absorption spectra recorded in a deaerated mixed aqueous–organic solvent at pH ~ 11 containing $1 \times 10^{-3} \text{ mol dm}^{-3}$ of *o*-HOBP and *m*-HOBP is shown in Figure 8. It is seen that at pH (~ 11) a strong transient absorption grows within about 40 μs in the 600 nm region. It is interesting to see that, unlike in the case of *p*-HOBP, when phenolic H is removed (in alkaline solution), dimethyl ketyl radical is able to reduce *o*- and *m*-HOBP giving a transient absorbing at ~ 600 nm. These

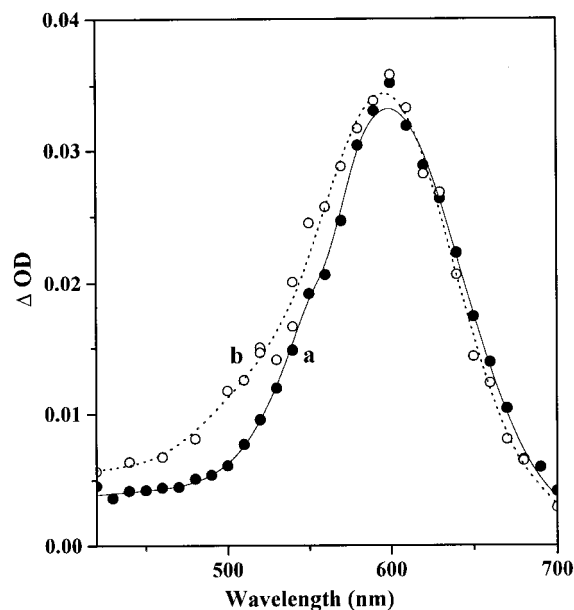
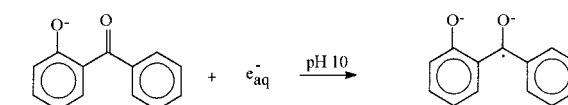
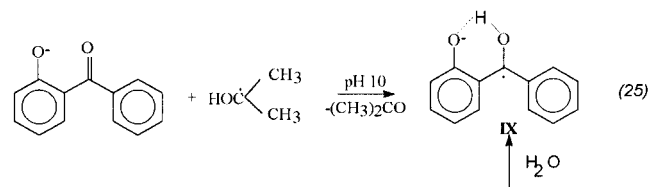
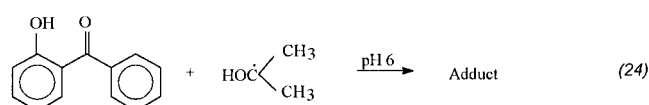


Figure 8. Transient absorption spectra recorded at 45 μs in deaerated mixed aqueous organic solvent at pH 11, containing $1 \times 10^{-3} \text{ mol dm}^{-3}$ *o*-HOBP (a) and *m*-HOBP (b).

SCHEME 5



spectra are very similar to the radical anion spectra obtained at the same pH through electron reaction.

The reaction rates were evaluated by following the growth kinetics at 600 nm. From the pseudo-first-order growth rates, the second-order rate constant for the reduction reaction was evaluated to be $8 \times 10^7 \text{ dm}^3 \text{ mol}^{-1} \text{ s}^{-1}$ and $8.5 \times 10^7 \text{ dm}^3 \text{ mol}^{-1} \text{ s}^{-1}$ for the *ortho*- and the *meta*- derivatives, respectively. In general, electron-transfer processes are fast ($k = 10^9$ – $10^{10} \text{ dm}^3 \text{ mol}^{-1} \text{ s}^{-1}$) and take about 300 ns for completion at the concentration of the solute used ($1 \times 10^{-3} \text{ mol dm}^{-3}$). Thus, the above rate constant values suggest another slow reaction channel for the reaction. This could be an H atom transfer from the isopropyl alcohol radical to the *o*-HOBP giving rise to the ketyl radical which is stabilized by hydrogen bonding to give species **IX** (reaction 25). It can be seen that the transient spectrum recorded for species **IX** through electron reaction (Figure 4) is in good agreement with the present one. The reactions can be represented as in Scheme 5.

In conclusion, the technique of pulse radiolysis has been used to study the complex reactions that follow electron addition to hydroxybenzenones. Various radical species involved have been spectrally characterized, and their kinetic and pK_a values

have been evaluated. The subtle differences observed for *p*-, *o*-, and *m*- derivatives have been explained. Reduction of HOBP's was also studied using dimethyl ketyl radicals as reductants in mixed water–acetone–2-propanol solvents. These radicals have been found to react via adduct formation with the HOBP's, whereas H atom transfer reactions have been identified in the reactions with ⁻OBP's.

References and Notes

- (1) (a) Wagner, P. J. *Top. Curr. Chem.* **1976**, *66*, 1. (b) Wagner, P. J.; Park, B. S. *Org. Photochem.* **1991**, *11*, 227.
- (2) Scaiano, J. C. *J. Photochem.* **1973**, *2*, 81.
- (3) Cohen, S. G.; Parola, A.; Parsons, G. H. *Chem. Rev.* **1973**, *73*, 141.
- (4) Wagner, P. J.; Leavitt, R. A. *J. Am. Chem. Soc.* **1973**, *95*, 3669.
- (5) Griller, D.; Howard, J. A.; Marriott, P. R.; Scaiano, J. C. *J. Am. Chem. Soc.* **1981**, *103*, 619.
- (6) Wagner, P. J.; Truman, R. J.; Scaiano, J. C. *J. Am. Chem. Soc.* **1985**, *107*, 7093.
- (7) Wagner, P. J.; Truman, R. J.; Puchalski, A. E.; Wake, R. *J. Am. Chem. Soc.* **1986**, *108*, 7727.
- (8) Wagner, P. J. *Acc. Chem. Res.* **1971**, *4*, 5383.
- (9) Wagner, P. J.; Thomas, M. J.; Harris, E. *J. Am. Chem. Soc.* **1976**, *98*, 7675.
- (10) Das, P. K.; Encinas, M. V.; Scaiano, J. C. *J. Am. Chem. Soc.* **1981**, *103*, 4154.
- (11) Leigh, W. J.; Lathioor, E. C.; St. Pierre, M. J. *J. Am. Chem. Soc.* **1996**, *118*, 12339.
- (12) Naguib, Y. M. A.; Steel, C.; Cohen, S. G.; Young, M. A. *J. Phys. Chem.* **1987**, *91*, 3033.
- (13) Bobrowski, K.; Marciniak, B.; Hug, G. L. *J. Am. Chem. Soc.* **1992**, *114*, 10279.
- (14) (a) Peters, K. S.; Lee, J. *J. Phys. Chem.* **1993**, *97*, 3761. (b) Simon, J. D.; Peters, K. S. *J. Am. Chem. Soc.* **1981**, *103*, 6403. (c) Simon, J. D.; Peters, K. S. *J. Am. Chem. Soc.* **1982**, *104*, 6542. (d) Simon, J. D.; Peters, K. S. *J. Phys. Chem.* **1983**, *87*, 4855.
- (15) Gramain, J. C.; Remuson, R. *J. Org. Chem.* **1985**, *50*, 1120.
- (16) (a) Wagner, P. J.; Leavitt, R. A. *J. Am. Chem. Soc.* **1970**, *92*, 5806. (b) Wagner, P. J.; Lam, H. M.-H. *J. Am. Chem. Soc.* **1980**, *102*, 4167. (c) Wagner, P. J.; Puchalski, A. E. *J. Am. Chem. Soc.* **1978**, *100*, 5948. (d) Wagner, P. J.; Puchalski, A. E. *J. Am. Chem. Soc.* **1980**, *102*, 6177. (e) Wagner, P. J.; Kemppainen, A. E.; Schott, H. N. *J. Am. Chem. Soc.* **1973**, *95*, 5604. (f) Wagner, P. J.; Siebert, E. J. *J. Am. Chem. Soc.* **1981**, *103*, 7329.
- (17) (a) Porter, G.; Suppan, P. *Trans. Faraday Soc.* **1966**, *62*, 3375. (b) Porter, G.; Suppan, P. *Trans. Faraday Soc.* **1965**, *61*, 1664.
- (18) Berger, M.; McAlpine, E.; Steel, C. *J. Am. Chem. Soc.* **1978**, *100*, 5147.
- (19) Wolf, W. M.; Brown, R. E.; Singer, L. A.; *J. Am. Chem. Soc.* **1977**, *99*, 526.
- (20) Aspari, P.; Ghoneim, N.; Haselbach, E.; Von Raumer, M.; Suppan, P.; Vauthey, E. *J. Chem. Soc., Faraday Trans.* **1996**, *92*, 1689.
- (21) (a) Beckett, A.; Porter, G. *Trans. Faraday Soc.* **1963**, *59*, 2038. (b) Ghoneim, N.; Monbelli, A.; Pilloud, D.; Suppan, P. *J. Photochem. Photobiol. A: Chem.* **1996**, *94*, 145.
- (22) Bhasikuttan, A. C.; Singh, A. K.; Palit, D. K.; Sapre, A. V.; Mittal, J. P. *J. Phys. Chem. A* **1998**, *102*, 3470.
- (23) Hoshino, M. *J. Phys. Chem.* **1987**, *91*, 6385.
- (24) Merritt, C.; Scott, G. W.; Gupta, A.; Yavrouian, A. *Chem. Phys. Lett.* **1980**, *69*, 169.
- (25) Hou, S.; Hetherington, W. M., III; Korenowski, G. M.; Eisenthal, K. B. *Chem. Phys. Lett.* **1979**, *68*, 282.
- (26) McGarry, P. F.; Jockusch, S.; Fujiwara, Y.; Kaprinidis, N. A.; Turro, N. J. *J. Phys. Chem.* **1997**, *101*, 764.
- (27) Lamola, A. A.; Sharp, L. J. *J. Phys. Chem.* **1966**, *70*, 2634.
- (28) Adams, G. E.; Baxandale, J. H.; Boag, J. W. *Proc. R. Soc., Ser. A.* **1964**, *277*, 549.
- (29) Bensasson, R. V.; Land, E. J.; Truscott, T. G. *Flash Photolysis and Pulse Radiolysis*; Pergamon Press: Oxford, UK, 1983.
- (30) (a) Hayon, E.; Ibata, T.; Lichtin, N. N.; Simic, M. *J. Phys. Chem.* **1972**, *76*, 2072. (b) Keene, J. P.; Land, E. J.; Swallow, A. J. *J. Am. Chem. Soc.* **1965**, *87*, 5284.
- (31) Guha, S. N.; Moorthy, P. N.; Kishore, K.; Naik, D. B.; Rao, K. N. *Proc. Indian Acad. Sci (Chem. Sci.)* **1989**, *99*, 261.
- (32) Baxandale, J. H., Bussi, F., Eds. *Study of Fast Processes and Transient Species in Pulse Radiolysis*; Reidel: Boston, MA, 1982; (a) p 49; (b) p 297.
- (33) Land, E. J.; Mukherjee, T.; Swallow, A. J.; Bruce, J. M. *J. Chem. Soc., Faraday Trans. 1* **1983**, *79*, 391.
- (34) Spinks, J. W. T.; Wood, R. J. *An Introduction to Radiation Chemistry*; Wiley-Interscience Publication: New York, 1990; (a) p 262; (b) p 327.
- (35) (a) Pal, H.; Palit, D. K.; Mukherjee, T.; Mittal, J. P. *Radiat. Phys. Chem.* **1992**, *40*, 529. (b) Pal, H.; Palit, D. K.; Mukherjee, T.; Mittal, J. P. *J. Chem. Soc., Faraday Trans.* **1991**, *87*, 1109.
- (36) Land, E. J. *Proc. R. Soc., Ser. A* **1968**, *305*, 457.
- (37) (a) Demeter, A.; Berces, T. *J. Phys. Chem.* **1991**, *95*, 1228. (b) Naguib, Y. M. A.; Steel, C.; Cohen, S. G. *J. Phys. Chem.* **1988**, *92*, 6574.
- (38) Asmus, K.-D.; Henglein, A.; Wigger, A.; Beck, G. *Ber. Bunsen-Ges. Phys. Chem.* **1966**, *70*, 756.
- (39) Tripathi, G. N. R. *J. Phys. Chem.* **1998**, *102*, 2388.
- (40) Naik, D. B.; Dwibedy, P.; Dey, G. R.; Kishore, K.; Moorthy, P. N. *J. Phys. Chem. A* **1998**, *102*, 684.